# CrystEngComm



### **HIGHLIGHT**

View Article Online



Cite this: CrystEngComm, 2025, 27, 3643

Received 24th March 2025, Accepted 28th April 2025

DOI: 10.1039/d5ce00311c

rsc.li/crvstengcomm

# Recent multifunctional applications of AIE-MOF/ **COF** porous materials

Siwen Liu, a Guijie Liang, a Song Wang (1)\*\* and Qingsong Hu\*\*\*

Luminescent materials play a crucial role in applications such as lighting, displays, sensing, and bio-imaging. However, their performance is often hindered by aggregation-caused quenching (ACQ). The discovery of aggregation-induced emission (AIE) in 2001 provided a breakthrough, utilizing AIE luminogens (AIEgens) that exhibit strong emission in the aggregated state due to restricted intramolecular motion (RIM). Unfortunately, for porous materials such as metal-organic frameworks (MOFs) and covalent organic frameworks (COFs), which are commonly used in gas storage, separation, and catalysis, their luminescence is often suppressed by strong  $\pi$ - $\pi$  interactions, resulting in ACQ. Integrating AlEgens into MOFs and COFs overcomes this limitation, creating luminescent porous polymers with enhanced optical and electronic properties through linker or metal center modifications. Furthermore, hybridizing MOFs and COFs unlocks additional structural and luminescence improvements, broadening their potential in advanced technologies. This review explores the versatile applications of AIE-MOF/COF materials, particularly in optoelectronic devices, sensing, biomedicine, and photocatalysis. We highlight recent advancements in their luminescence properties, structural functionalization, and future research directions, offering insights into their design and multifunctional applications. Finally, we discuss challenges related to their luminescence and propose strategies to enhance their performance for broader practical implementation.

### 1. Introduction

Luminescent materials can emit photons through the process of excitation-deexcitation. They are known for their high efficiency, stability, and controllability, with applications in lighting, displays, sensing, and bio-imaging. 1-4 These materials hold great potential in new display technologies, high-efficiency lighting, biomedicine, and environmental protection, making them essential to modern society. Luminescent materials exist primarily in liquid and solid states, with a few in the gaseous form. Traditional luminescent molecules exhibit strong emission in isolation, but their aggregation often triggers aggregation-caused quenching (ACQ).5-7 ACQ arises from the close stacking of large planar  $\pi$ -complexes, which diminishes luminescence efficiency and restricts practical applications. In contrast, the aggregation-induced emission (AIE) phenomenon, first introduced by Ben Zhong Tang et al. in 2001, overcomes this limitation by enhancing luminescence upon aggregation.8

AIE luminogens (AIEgens) exhibit weak or no emission in dilute solutions but emit strongly in the aggregated state. The most widely accepted mechanism for this phenomenon is restricted intramolecular motion (RIM). 1,9,10 Over the years, various AIEgens have been developed, offering high quantum yields, strong stability, resistance to interference, and a broad range of adjustable wavelengths. These features make them highly valuable for applications in light-emitting devices, sensing, and bio-imaging. 11-13

Porous materials-such as metal-organic frameworks (MOFs), covalent organic frameworks (COFs), hydrogenbonded organic frameworks (HOFs), and amorphous porous organic polymers (POPs)-are widely studied due to their potential in scientific research and engineering. 14-17 Among them, MOFs and COFs are particularly notable due to their high surface areas and tunable pore structures, making them ideal for applications in gas storage, separation, and catalysis. MOFs offer precise control over pore size, chemical properties, and structural morphology through the selection of different metal centers and organic ligands. In contrast, COFs form stable, well-defined pore networks via covalent bonding of organic units, providing excellent thermal stability and chemical resistance. Tailoring the structures of MOFs and COFs by designing specific metal ions, ligands, or organic components further enhances their functional versatility, enabling applications in catalysis, drug delivery,

<sup>&</sup>lt;sup>a</sup> Hubei Key Laboratory of Low Dimensional Optoelectronic Materials and Devices, Hubei University of Arts and Science, Xiangyang 441053, China. E-mail: wangsong1984@126.com

<sup>&</sup>lt;sup>b</sup> Advanced Membranes and Porous Materials Center (AMPMC) & KAUST Catalysis Center (KCC), Division of Physical Science and Engineering (PSE), King Abdullah University of Science and Technology (KAUST), Thuwal 23955-6900, Kingdom of Saudi Arabia. E-mail: qingsong.hu@kaust.edu.sa

and environmental treatment. However, strong  $\pi$ - $\pi$ interactions in porous frameworks often lead to ACQ, limiting their luminescence efficiency. To overcome this challenge, integrating AIEgens into porous skeletons has emerged as a powerful strategy for developing novel luminescent porous polymers, effectively overcoming the limitations of conventional luminescent materials.

In recent years, the construction of MOFs and COFs using AIEgens has garnered significant attention. 21-26 This integration offers several unique advantages, such as tunable optical and electronic properties, controlled fluorescence emission, and structural versatility and functionalization. While most research on AIE-MOF/COF materials has focused on sensing and detection, their potential extends far beyond these fields. 27-33 In the field of sensing, Wei et al. reviewed the significant potential of AIE-MOFs as various sensors.<sup>34</sup> Cheng et al. focused on food safety and systematically summarized the application of luminescent porous materials based on AIE in detecting harmful pollutants,35 while Zhu et al. elaborated on the strategies for AIE-MOF construction and performance control, with structural design as the core.23 Dalapati et al. described the design, synthesis, and functionalization of AIE porous polymers based on organic ligands.<sup>36</sup> However, the exploration of AIE-MOF/COF materials in this emerging field is still limited, and further research is urgently needed. This review explores the diverse applications of AIE-MOF/COF materials, particularly in optoelectronic biomedicine, devices, sensing, and photocatalysis, as shown in Fig. 1, with a focus on recent advancements luminescence properties multifunctional applications. We will examine the structural functionalization of AIE-MOF/COF materials to guide the

next-generation multifunctional design of Additionally, we will discuss existing challenges related to their luminescence properties and applications, offering insights into future research directions in chemistry, physics, and materials science.

### 2. Basic properties of AIE-MOF/COF porous materials

#### 2.1 AIE effect and its mechanisms

When discussing the AIE effect, it is essential to first address the phenomenon of ACO. Since Förster's discovery of the concentration burst effect in 1954, ACQ has been extensively studied, and its photophysical processes and mechanisms are well understood.5 ACQ occurs when aromatic rings of adjacent luminescent groups, particularly those with disc- or rod-like shapes, undergo strong intermolecular  $\pi$ - $\pi$  stacking interactions.<sup>1,9</sup> Such aggregation leads to non-radiative decay pathways, resulting in fluorescence quenching. ACO is a common but detrimental effect in luminescent materials.

In contrast, the AIE phenomenon represents an alternative photophysical process in which chromophores exhibit enhanced fluorescence upon aggregation. For example, hexaphenylsilane (HPS) remains non-emissive in its isolated molecular state but displays strong luminescence when aggregated.8,37 The most widely accepted mechanism underlying AIE is the RIM model, which consists of restricted intramolecular rotation (RIR) and restricted intramolecular vibration (RIV), as shown in Fig. 2(A). The fluorescence of tetraphenylethylene (TPE), a classic AIEgen, is induced or restored through the suppression of molecular rotation and the disruption of intermolecular  $\pi$ - $\pi$  stacking interactions.

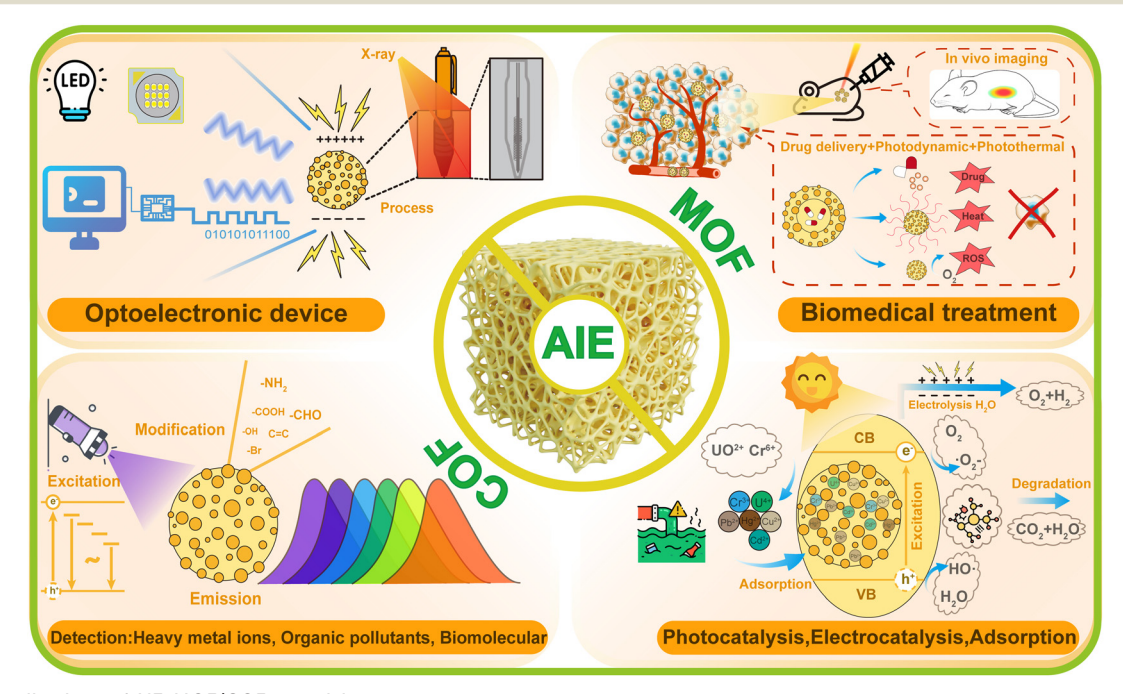


Fig. 1 The applications of AIE-MOF/COF materials

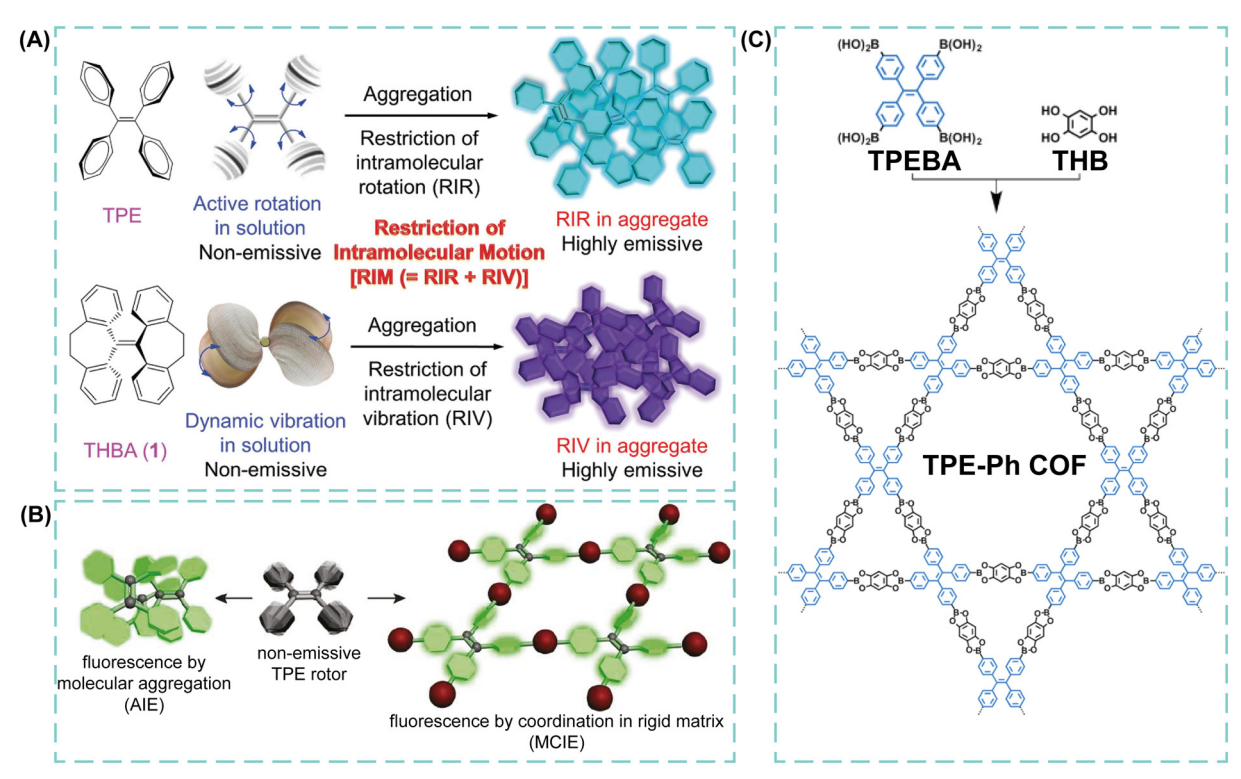


Fig. 2 (A) Main mechanism of the AIE phenomenon. Reproduced with permission from ref. 9. Copyright 2014 Wiley-VCH. (B) Turning on fluorescence in the TPE rotor by aggregation and coordination in a rigid MOF matrix (MCIE). Reproduced with permission from ref. 42. Copyright 2011 American Chemical Society. (C) Synthesis of the TPE-Ph COF from TPEBA and THB. Reproduced with permission from ref. 62. Copyright 2016 American Chemical Society.

Similarly, the AIE behaviour of helical molecules such as HPS can be attributed to the RIR process. However, for luminophores with highly flexible molecular segments, the AIE effect can also be explained by RIV. For instance, in THBA (Fig. 2(A)), the AIE effect arises in part from the limitation of vibrational motion in flexible molecular segments, thereby reducing non-radiative exciton energy dissipation.9

Besides RIR and RIV, researchers have explored additional governing AIE, including mechanisms J-aggregate formation,  $^{38,39}$  E/Z isomerization,  $^{40}$  twisted intramolecular charge transfer (TICT),41,42 and excited-state intramolecular proton transfer (ESIPT).43,44 These mechanisms describe various excited-state molecular motions and complement rather than contradict the RIM model. The restricted motion of molecules makes AIEgens highly suitable for integration into porous frameworks. In porous crystalline materials such as MOFs and COFs, which feature rigid skeletons and periodic pore structures, AIEgens can be incorporated either as structural components of the framework or as guest molecules within the pores.

#### 2.2 Construction and performance of AIE-MOFs

The key factors in constructing AIE-MOFs are the choice of organic ligands and metal ions. Organic ligands serve as the primary framework, with commonly used ones including

tetraphenylethylene (TPE), 4',4",4"'-(ethene-1,1,2,2-tetrayl) tetrabiphenyl-4-carboxylic acid (H4TCPE), etc., partly listed in Table 1. The first example of AIEgens in MOF materials involved the immobilization of functionalized TPE ligands, which prevented chromophore stacking and enabled fluorescence turn-on.45 In another study, tetrakis(4carboxyphenyl)ethylene (TCPEE) was coordinated with d10 metal ions to form luminescent MOFs (Fig. 2(B)). Despite the large intermolecular distances induced by coordination with metal ions, the fluorescence quantum yield of these MOFs remained relatively low due to the partial freedom of benzene ring rotation in TCPEE. Optimization of this system through deuteration of the TPE core significantly enhanced fluorescence efficiency.46 Solid-state 2H and 13C NMR along with variable-temperature experiments, diffraction and density functional theory (DFT) calculations, were employed to investigate the dynamics of the benzene ring in TPE-based MOFs. The findings revealed that both ethylene C=C twisting and benzene ring torsion influence fluorescence emission, with the former potentially acting as a gating mechanism for the latter. This study provided valuable insights into the relationship between molecular dynamics and fluorescence efficiency, offering a strategy to modulate activation barriers and optimize novel AIE-MOF materials. Recent research has extensively focused on TPE and its derivatives. By modifying ligand structures—such introducing different substituents

 Table 1
 Some of the organic molecules used to construct AIE-MOF/COF materials

I SOTTIE OF LITE OF STATES THORECE	SOTTE OF THE ORGANIC MORCULES USED TO CONSTRUCT AIE-MOT/COT MARKINS				
Molecule	Name	Ref.	Molecule	Name	Ref.
	Tetraphenylethylene	87, 96, 107 87, 96, 107		4,4',4", 4"-(Dibenzo[g,p]chrysene)tetrakisaniline (TPTBN)	32, 67
Z Z	4,4'-(((9 <i>H</i> -Fluoren-9-ylidene)methylene) bis(4,1-phenylene))dipyridine	48		2,2'-Bipyridine-4,4'-dicarboxylic acid (H2L)	114
	Tetraaldehyde tetrastyrene	66, 83		4,4',4",4"-(Porphyrin-5,10,15,20-tetrayl) tetra-aniline (TAPP)	108
HO OH	4,4'-(Pyrene-1,6-diyl)dibenzoic acid (H <sub>2</sub> PDBA)	49		4',4"',4"'',4"''-(Ethene-1,1,2,2 tetrayl) tetrakis([[1,1'-biphenyl]-4-carbaldehyde)) (ETBC)	71, 75, 77
O T TO	$4,4',4'',4''$ -(Quinoxaline-2,3,6,7-tetrayl) tetrabenzoate ( $H_4TCPQ$ )	120	NO N	4,4',4",4"-(Ethene-1,1,2,2-tetrayl) tetraaniline	62, 63, 64, 74, 111
	1,3,6,8-Tetra(4-carboxyphenyl)pyrene (H4TBAPy)	104, 106		4-(2,4,5-Tripyridin- $4$ -ylphenyl)pyridine (TPB)	24

CrystEngComm

45, 46, 91, 93, 94, 117 94, 117 47, 50, 56, 57, 72, 99, 105 Ref. 100 1,1,2,2-Tetra(4-carboxylphenyl)ethylene (TCPEE) bis([[2,2':6',2"-terpyridine]-5,5"-dicarbaldehyde]) tetrakis([1,1'-biphenyl]-3-carboxylic acid) 4',4"',4""',4""''-(Ethene-1,1,2,2-tetrayl) 4',4""-(1,4-Phenylene) (H4TCPE) Name Molecule 27, 30, 33, 118, 119 Ref. tetrakis([1,1'-biphenyl]-3,5-dicarboxylic acid) 1,1,2,2-Tetrakis(4-pyrazolylphenyl)ethene (Py-TPE) 2,3,5,6-Tetrakis(4-carboxyphenyl)pyrazine (H<sub>4</sub>TCPP) 4',4"',4"",4""''-(Ethene-1,1,2,2-tetrayl) HETTB Molecule

conjugation system—the emission peak positions can be fine-tuned, while variations in framework connectivity influence the degree of motion restriction in AIEgens, thereby controlling their luminescence properties. 47-50

Another approach involves embedding AIEgen molecules within MOF voids to restrict their movement, simplifying MOF design while enabling the AIE effect. Dong et al. demonstrated that tuning the ratio of TPE-based organic linkers in a MOF system effectively controlled the number of AIE molecular rotors (dynamic benzene rings), resulting in highly tunable photophysical properties with a linear dependence on the linker ratio.<sup>51</sup> Increasing the number of AIE molecular rotors enhanced the sensing sensitivity of dynamic MOFs, highlighting the functional versatility of these materials. Many other studies on AIEgen-modified MOF pores further confirm the modifiability and tunability of MOFs. 52-55

Besides ligand design, the selection of metal ions or clusters is crucial, as they form stable coordination bonds with organic ligands and contribute to diverse coordination modes. This flexibility allows for the formation of various topologies while maintaining charge balance for structural stability. Zhou's group developed a novel tetraphenylenebased zirconium MOF exhibiting bright blue fluorescence emission at 470 nm with a remarkably high quantum yield of 99.9  $\pm$  0.5% under an Ar atmosphere. <sup>56</sup> They later synthesized a PCN-128W MOF by varying the metal nodes, which displayed reversible piezoelectric fluorescence discoloration, shifting from white to yellow under mechanical stress.<sup>57</sup> Similarly, Guo et al. synthesized two variants, Sr-ETTB and Co-ETTB, by incorporating different metal nodes with the same ligand. Sr-ETTB exhibited strong fluorescence at 470 nm ( $\Phi_{\rm F}$  = 54.6%) with a highly sensitive and reversible luminescence response to pressure and temperature. In contrast, replacing Sr2+ with Co2+ yielded non-emissive Co-ETTB ( $\Phi_{\rm F}$  = 0.14%) due to primary ligand-to-metal and secondary ligand-to-ligand charge transfer transitions.<sup>58</sup> Not only that, the recent construction of AIE MOFs using AIE-type metal nanoclusters has significantly expanded the variety of AIE-MOFs that can be created. 59-61

#### 2.3 Construction and performance of AIE-COFs

COFs have also garnered significant attention as luminescent materials due to their stable covalent bonding, intrinsic porosity, low backbone density, and high structural stability. Unlike MOFs, COFs lack metal ions or clusters, relying entirely on covalent bonds between organic monomers. This structural difference makes the synthesis of AIE-COFs more challenging. Like conventional COFs, AIE-COFs can be classified into 2D-COFs and 3D-COFs based on their dimensionality.

2D-luminescent MOFs often suffer from the ACO effect due to face-to-face  $\pi$ - $\pi$  stacking, which leads to fluorescence quenching. Incorporating AIEgens into 2D-COFs is one of the most effective strategies to overcome ACQ and achieve high

Fable 1 (continued)

emissivity. Early on, Zhao's group successfully synthesized a series of 2D-COFs using TPE-based organic ligands, laying the theoretical foundation for AIE-COF synthesis. 62-64 Dalapati et al. synthesized high-emissivity 2D TPE-Ph COFs (Fig. 2(C)) using vinyl-functionalized TPE units. They successfully mitigated the fluorescence quenching effect caused by interlayer  $\pi$ - $\pi$  stacking through the introduction of an AIE mechanism. 65 By incorporating AIE-active units at the vertices of polygonal frameworks, they achieved crystalline porous COFs with periodic  $\pi$ -stacked columnar AIE arrays. These arrays enhance luminescence performance through the combined effects of strong intra-layer covalent bonding and inter-layer non-covalent  $\pi$ - $\pi$  interactions. Notably, these materials exhibit excellent quantum yields and function as highly sensitive sensors capable of detecting ammonia at sub-ppm levels. Since then, various 2D-COFs based on AIE ligands have been designed for diverse applications. 66-68

To further suppress ACQ, constructing 3D-COFs is another promising approach. Lin et al. reported the first pyrene-based 3D-Py-COF with a PtS-type topology, carefully selecting the precursor geometry and connectivity. This COF exhibited a narrow pore size distribution, high specific surface area, and selective CO2 adsorption over N2. Due to its isolated pyrene units, it became the first fluorescent 3D-COF capable of detecting explosives.<sup>69</sup> Lin's group later synthesized two porphyrin-based 3D-COFs that demonstrated significant photocatalytic activity. 70 Ding et al. further expanded on this work by synthesizing a TPE-based 3D-COF with a sevenfold interspersed PtS topology in the P2/c space group. This material emitted yellow fluorescence upon excitation, with a photoluminescence quantum yield (PLQY) of 20%. Additionally, white-light LEDs (WLEDs) were fabricated by simply coating a 3D-TPE-COF onto commercial blue LEDs, maintaining stability after 1200 hours of natural aging.<sup>71</sup> Despite these advancements, research on AIEgen-based 3D-COFs remains limited. The development of multifunctional AIEgen-based 3D-COFs is particularly challenging due to their intricate structures and unique properties, making this an exciting yet demanding area for future exploration.

# 3. Applications of AIE-MOF/COF porous materials

As a unique class of luminescent materials different from traditional ones, AIEgens exhibit remarkable luminescence properties in the aggregated state, characterized by high quantum yields and excellent photostability. To fully harness these properties, it is crucial to restrict the molecular motion of AIEgens, a goal effectively achieved through MOFs or COFs. These porous, rigid structures serve as ideal scaffolds, effectively limiting the intramolecular motions of AIEgens and thereby enhancing their luminescence.<sup>23</sup> Moreover, finetuning the structure of AIE-based ligands enables precise control over both the color and intensity of the emitted light. Additionally, selecting different metal nodes within these frameworks can further modulate the luminescence lifetime

and stability. A key advantage of MOF/COF materials lies in their intrinsic porosity, which not only facilitates the encapsulation of AIEgens but also allows for the integration of other functional molecules. This integration of advantages endows these materials with exceptional multifunctionality, making them highly suitable for applications in optoelectronics, sensing, biomedicine, and catalysis. The following sections provide an overview of recent advancements in AIE-MOF/COF research, highlighting key developments across various aspects.

# 3.1 Advances in AIE-MOF/COF materials for optoelectronic applications

AIEgens have been extensively investigated for light-emitting display applications. However, the luminescence efficiency of MOFs and COFs incorporating AIE properties still requires further enhancement, and their potential in emerging optoelectronic applications still needs further exploration. Recent studies have made significant progress in addressing these challenges, demonstrating novel strategies for optimizing luminescence performance and broadening the scope of AIE-MOF/COF applications in optoelectronics.

Yuan et al. recently reported the design and synthesis of a novel columnar MOF framework constructed from H4TCPE, ions  $(Zn^{2+}),$ and N,N'-di(4-pyridyl)-1,4,5,8zinc naphthalenetetracarboxydiimide (DPNI).72 The resulting structure, Zn-TCPE-DPNI, exhibits a dual interpenetration topology (Fig. 3(A)). Within this framework, efficient charge transfer occurs between H<sub>4</sub>TCPE and Zn<sup>2+</sup>, while the RIM of the H<sub>4</sub>TCPE ligand enhances the AIE effect, leading to highly luminescent MOFs. A key feature of Zn-TCPE-DPNI is its tunable NLO response, achieved by varying the excitation wavelength of a femtosecond laser from 900 to 1500 nm. The MOF single crystals exhibit multiple NLO effects, including two-photon absorption, three-photon absorption, and third harmonic generation (THG). Notably, under 1500 nm excitation, pure THG was observed with an effective NLO constant of  $2.9 \times 10^{-12}$  esu—significantly higher than that of conventional materials such as quartz. This work presents a new strategy for designing photoluminescent MOF crystals with controllable NLO properties, offering promising prospects for advanced optoelectronic and biophotonic device applications.

Recent studies have highlighted the importance of suppressing nonradiative decay to enhance the luminescence of AIE-COFs. <sup>73</sup> Liu *et al.* proposed a dual-regulation strategy that combines interlayer spacing expansion and intramolecular rotation restriction, resulting in a PLQY of 21.22% in a TPAZ-TPE-COF and enabling efficient Fe<sup>2+</sup> sensing and white light emission. <sup>74</sup> In contrast, Wan *et al.* focused on modulating linker conjugation and flexibility. <sup>75</sup> By employing weakly conjugated hydrazone linkers and a flexible AIE-active TFBE core, they constructed Hz-COFTFBE-ODH with a higher PLQY of 26.28%, enhanced solid-state emission, and practical applications in both WLEDs and

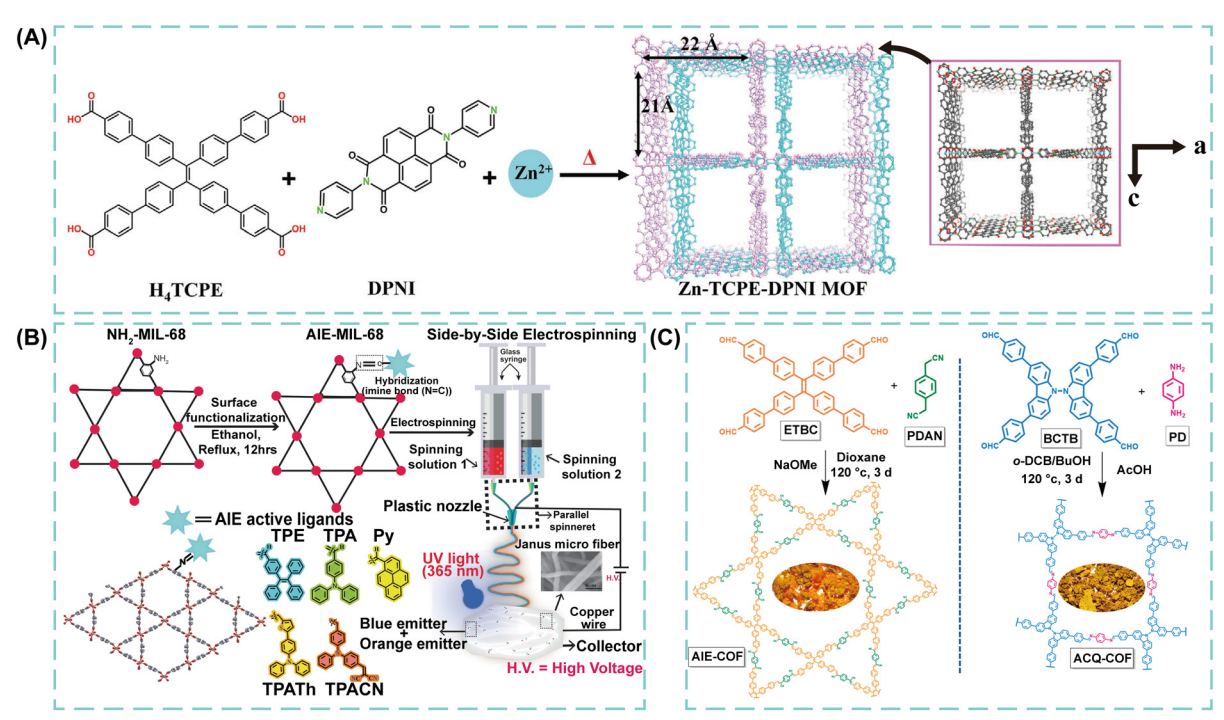


Fig. 3 (A) Synthesis of a photoluminescent AIE-MOF with tunable nonlinear optical (NLO) response from H<sub>4</sub>TCPE and DPNI. Reproduced with permission from ref. 72. Copyright 2024 Wiley-VCH. (B) A Janus-type white light-emitting AIE-MOF fiber composite prepared by bilateral electrospinning technology. Reproduced with permission from ref. 76. Copyright 2023 Wiley-VCH. (C) Adoption of an AIE-COF as a color converter for a high net data transfer rate. Reproduced with permission from ref. 77. Copyright 2024 American Chemical Society.

antibiotic sensing. While Liu's strategy emphasizes structural rigidity and packing control, Wan's work demonstrates the effectiveness of linker engineering in balancing  $\pi$ -conjugation and molecular motion. Together, these approaches underscore the versatility of AIE principles in COF design and provide complementary pathways toward high-performance luminescent materials. In addition, Kachwal et al. explored a hybrid approach to tuning the luminescence properties of AIE-MOFs by incorporating them into electrospun Janus microfibers.<sup>76</sup> Using post-synthetic modification, they introduced donor-acceptor (D-A) type AIEactive ligands into three different MOFs (NH2-UiO-66(Zr), NH<sub>2</sub>-MIL-53(Al), and NH<sub>2</sub>-MIL-68(In)) resulting in AIE-MOFs with emission spectra tunable across the visible range (Fig. 3(B)). When embedded in a polymer matrix, the fiber structure significantly enhanced the luminescence efficiency of the AIE-MOFs compared to their powdered form. Through bilateral electrospinning, the researchers fabricated Janustype white light-emitting AIE-MOF fiber composites with an impressive PLQY of 58%-double that of homogeneous fibers. Nevertheless, further studies are needed to explore the long-term photostability, thermal resistance, and large-area fabrication compatibility of these Janus AIE-MOF fibers. This approach highlights the potential of hybrid AIE-MOFs with Janus-type structures for efficient white light emission, paving the way for tunable, high-performance materials in optoelectronics, lighting, and displays.

In the field of optical wireless communication (OWC), Jindal synthesized AIE-COFs using the Knoevenagel condensation reaction.<sup>77</sup> The resulting AIE-COFs exhibited a significantly higher solid-state PLQY (39%) and a shorter luminescence lifetime (1 ns) compared to conventional ACQ-COFs (Fig. 3(C)). Importantly, the luminescence intensity and quantum yield of AIE-COFs increased in the aggregated state, enhancing their potential for OWC applications. With a -3 dB modulation bandwidth reaching nearly 200 MHz, AIE-COFs demonstrated superior performance compared to conventional materials. As a color converter, the material achieved a net data rate of 825 Mb s<sup>-1</sup>, surpassing traditional color conversion materials used in OWC systems. Compared to the 1.076 Gb s<sup>-1</sup> transmission rate and 65.7 MHz bandwidth of the TPE-based molecules integrated into the recent MOF used by Zhu,<sup>78</sup> it is more suitable for optical modulation applications that require a high-frequency response or low latency due to its higher modulation bandwidth.

These recent advancements highlight the growing potential of AIE-MOF/COF materials in optoelectronic applications. By leveraging their tunable luminescence properties, enhanced NLO responses, and improved efficiency in composite structures, researchers are pushing the boundaries of these materials in display technologies, optical communication, and beyond. AIE-MOF/COF materials offer multiple advantages, including low cost, straightforward synthesis, and high stability, making them highly promising for flexible optoelectronic devices. Future studies will further refine their design and integration into practical devices, unlocking new opportunities for high-performance optoelectronic and photonic systems.

# 3.2 AIE-MOF/COF materials for advanced sensing applications

Materials with AIE properties have been widely employed in various sensing applications due to their exceptional optical characteristics, including high sensitivity, selectivity, and rapid response. These materials have demonstrated remarkable performance in detecting metal ions, gases, volatile organic compounds (VOCs), and acid-base variations, including pH changes. Notably, AIE-MOF/COF materials exhibit enhanced luminescence signals due to the AIE effect, while their tunable structural features and pore sizes contribute to efficient and highly selective ion detection. Their fast and reversible optical response further ensures reliable and efficient detection. Roberts

The detection of inorganic ions is a critical aspect of chemical sensing, where AIE-MOF/COF composite materials have proven effective in improving detection efficiency. Recently, Zhang *et al.* developed a highly sensitive mercury ion (Hg<sup>2+</sup>) detection system by integrating 6-aza-2-thiothymine (ATT)-protected gold nanoclusters (AuNCs) with

cerium-based MOFs.<sup>82</sup> The researchers employed an electrostatic attraction strategy to assemble positively charged Ce-MOFs with negatively charged AuNCs, forming AuNC/Ce-MOF composites (Fig. 4(A)). In this system, the electrostatic interaction facilitated AuNC aggregation on the Ce-MOF surface, thereby enhancing the AIE effect. Simultaneously, the Ce-MOF structure restricted the movement of ATT ligands in the AuNCs, inducing the restriction of the RIM effect, which reduced non-radiative relaxation pathways and significantly enhanced fluorescence intensity. Upon the introduction of Hg<sup>2+</sup>, Ce-MOFs effectively increased the local Hg2+ concentration, triggering Au-Hg specific recognition and leading to fluorescence quenching. This resulted in a well-defined linear  $Hg^{2+}$ between concentration and relationship the fluorescence intensity, enabling highly sensitive detection with a broad dynamic range and a low detection limit. Besides Hg<sup>2+</sup> detection, AIE-MOF/COF materials have also been successfully applied for detecting a variety of metal ions, including Al3+ and Cu2+, through fluorescence-based sensing mechanisms.83-85

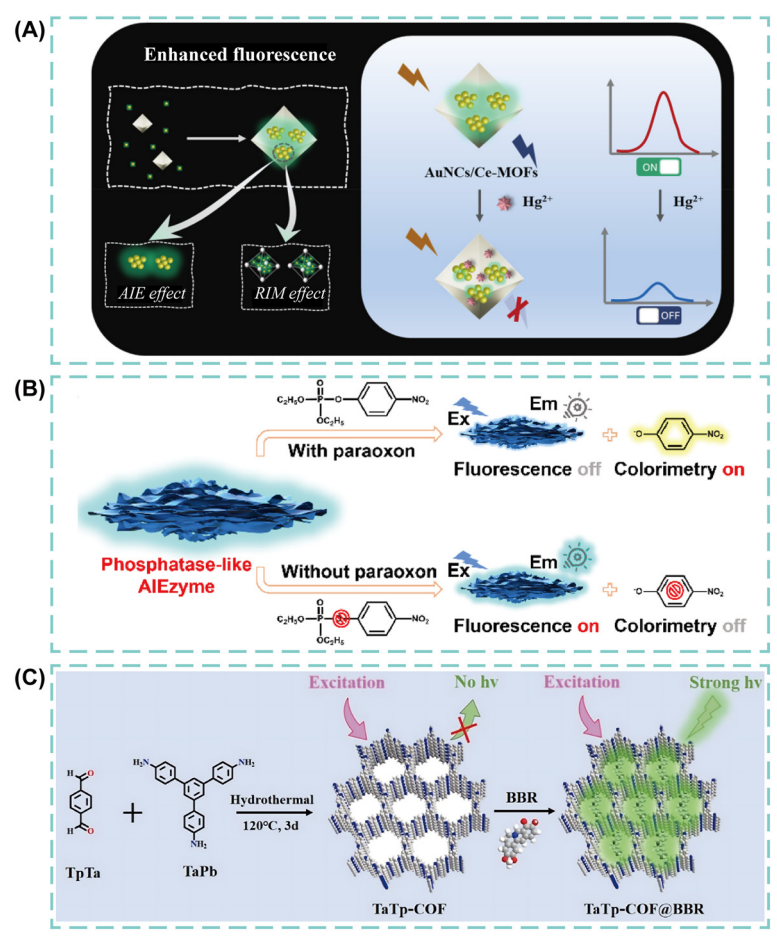


Fig. 4 (A) AuNC/Ce-MOF composites for the sensitive detection of mercury ions (Hg<sup>2+</sup>). Reproduced with permission from ref. 82. Copyright 2024 Elsevier. (B) A natural enzyme-free dual-mode colorimetric/fluorescence method for the detection of oxyphosphorus by Zr-based AIE MOFs. Reproduced with permission from ref. 91. Copyright 2025 Elsevier. (C) TaTp-COFs synthesized using TaPb and TpTa for the detection of BBR. Reproduced with permission from ref. 92. Copyright 2024 Elsevier.

In addition to metal ions, AIE-MOF/COF composites have shown great promise for detecting organic pollutants, including tetracycline antibiotics, nitro-containing explosives, pesticide residues, and other hazardous organic molecules.86-90 Zhu et al. developed an efficient detection method for organophosphorus compounds by synthesizing a zirconium-based MOF (Zr-MOF) composed of Zr4+ ions and the AIE-active ligand TCPEE. 91 This MOF topology effectively leverages the AIE mechanism, where the rigid framework of Zr4+ ions stabilizes TCPE, resulting in enhanced fluorescence and high phosphatase-like activity (Fig. 4(B)). The unique catalytic properties of the Zr-MOF hydrolysis of phosphate-containing enable selective compounds, including paraoxon, generating yellow p-nitrophenol via the Zr4+ active nodes. This process simultaneously affects the inherent fluorescence of TCPE, leading to a dual signal output combining colorimetric and fluorescence detection. Such cross-detection strategies improve detection accuracy and broaden the application scope of AIE-MOF materials in environmental monitoring and biochemical analysis. Similarly, Wang et al. synthesized a TaTp-COF for the detection of berberine (BBR).92 The COF structure significantly enhanced the fluorescence properties of BBR by restricting its free movement through weak hydrogen bonding interactions within the COF cavity (Fig. 4(C)). While the TaTp-COF itself exhibits negligible fluorescence in aqueous solution, the presence of trace amounts of BBR induces strong green fluorescence, enabling highly sensitive detection. In addition, Tang et al. constructed a Mn(III)-based AIE-MOF sensor that enables target-induced framework dissociation and fluorescence chlorpyrifos detection.<sup>93</sup> The for demonstrated strong AIE enhancement, high selectivity, and a low detection limit (3.79 ng mL<sup>-1</sup>), facilitating real-time monitoring of pesticide bioaccumulation in crops. To further enhance the sensing performance of MOFs, Jiang et al. constructed a dual-AIE MOF by combining two AIE-linkers, achieving a high quantum yield of 92.6%.94 This MOF enabled ultrasensitive and selective detection of the pesticide DCN (LOD = 123 ppb) through fluorescence quenching, with real-time visual sensing on fruits and soil and quantitative analysis via computer vision. In addition, recent sensing research on metal clusters,95 explosive detection,96 and biomedical macromolecules shows great promise. 97-99

Although AIE materials have been extensively developed for various sensing applications, their integration with porous frameworks such as MOFs and COFs significantly expands their functional capabilities. These hybrid materials exhibit enhanced selectivity, sensitivity, and stability in detecting both inorganic ions and organic pollutants, making them highly promising for environmental monitoring, chemical analysis, and biomedical applications. However, challenges remain in further improving detection sensitivity and selectivity, requiring continued advancements in material design and sensing strategies to unlock their full potential.

### 3.3 AIE-MOF/COF materials for biomedical applications

AIE materials have garnered significant attention in the biomedical field due to their ability to maintain bright and stable luminescence even at high concentrations or in aggregated states. 100-103 Through structural modifications and biocompatible designs, these materials have been successfully applied in cellular and in vivo imaging, biomolecular detection, drug delivery, therapeutic monitoring, and photodynamic and photothermal therapies, opening new avenues for precision medicine.

Electrochemiluminescence (ECL) is a widely recognized analytical technique due to its high sensitivity and low background interference, making it particularly valuable for clinical diagnostics and drug monitoring. There have been many recent advances in ECL materials based on AIE properties. 104,105 Hu et al. developed a dual-signal ECL immunosensor for detecting the biomarker serum amyloid A (SAA). 106 They synthesized an ECL sensor based on a lanthanide metal-organic framework (La-MOF), where 1,3,6,8-tetra(4-carboxybenzene)pyrene (H<sub>4</sub>TBAPy) served as the ligand and La<sup>3+</sup> as the central metal ion (Fig. 5(A)). This design effectively enhanced the ECL response by overcoming the inherently weak ECL intensity of the H<sub>4</sub>TBAPy ligand, thereby improving the quantum yield. When applied to detect SAA, the difference between the anodic and cathodic ECL signals showed a strong correlation with SAA concentrations ranging from 100 fg mL<sup>-1</sup> to 200 ng mL<sup>-1</sup>, with a detection limit of 24.5 mg mL<sup>-1</sup>. This approach provides a reliable method for detecting SAA in clinical samples. To advance AIE-based sensing, Li et al. developed a nanoconfined AIE-ECL system by embedding TPE into NH2-MIL-88, enhancing ECL efficiency via in situ catalysis. 107 This platform enabled smartphone-based, self-reporting detection of cardiac troponin I (cTnI) with ultrahigh sensitivity, highlighting its potential for point-of-care diagnostics.

In therapeutic applications, AIE-COFs have emerged as promising non-metallic thermotherapeutic agents. Zhang et al. synthesized three AIE-COF materials (TDTA-COF, BTDTA-COF, and BTDBETA-COF) and explored their use in hyperthermia therapy for suppressing malignant VAs. 108 These AIE-COFs directly modulated the stellate ganglion (SG) function and neural activity through local warming therapy, browning promoting white fat and alleviating neuroinflammatory conditions surrounding the (Fig. 5(B)). This, in turn, effectively suppressed ischemiainduced VAs, marking the first instance of an AIE-COF-based non-metallic thermotherapeutic approach for cardiac treatment. The study highlights the potential of AIE-COFs in neurocardiology and biomedical applications, providing new therapeutic strategies for reducing cardiac sympathetic overactivity. Recently, they effectively induced tertiary lymphoid structure (TLS) formation through an AIE-COF, creating a chronic inflammatory microenvironment, promoting high cytokine secretion, enhancing the effects of phototherapy, and recruiting and activating immune cells for

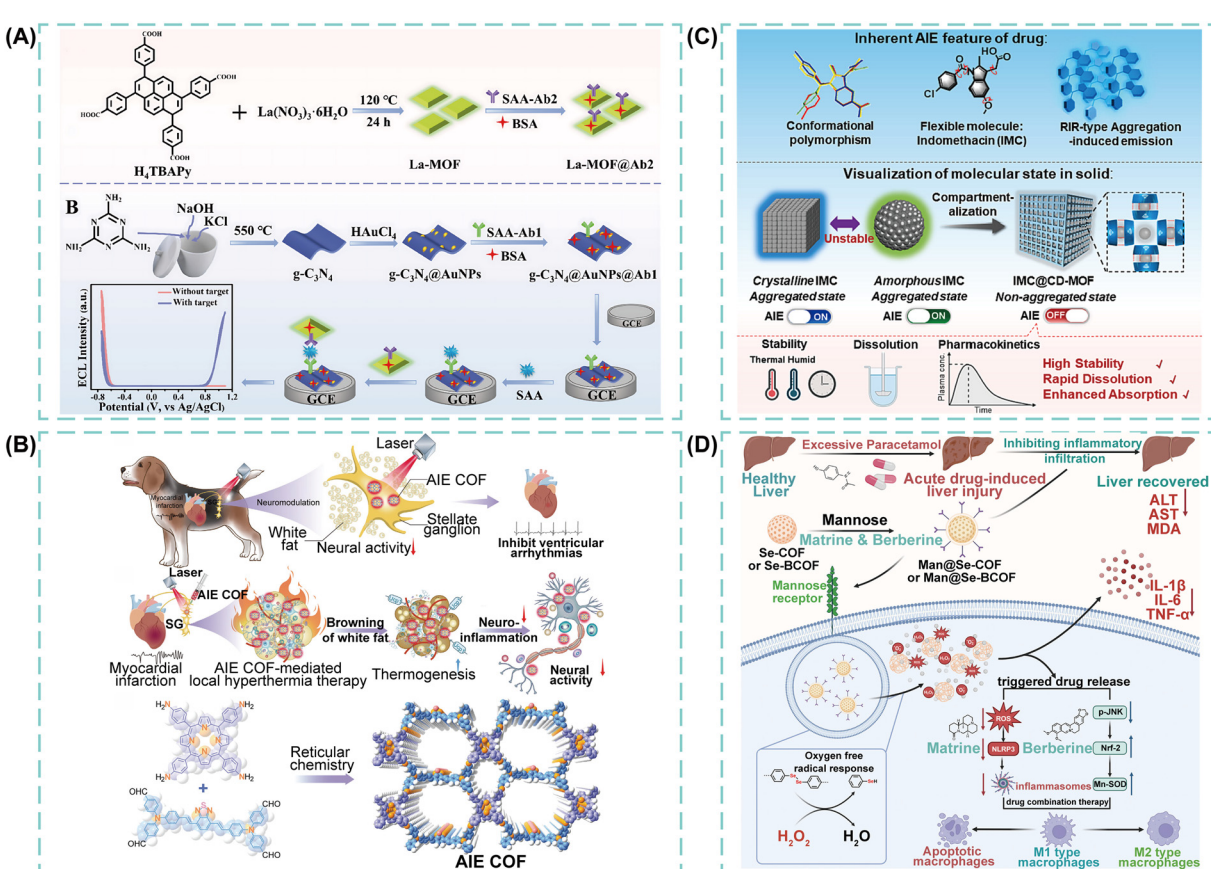


Fig. 5 (A) Detection of SAA using a La-AIE-MOF dual-signal ECL immunosensor. Reproduced with permission from ref. 106. Copyright 2025 Elsevier. (B) An AIE-COF non-metallic hyperthermia agent for the inhibition of ventricular arrhythmias (VAs). Reproduced with permission from ref. 108. Copyright 2023 Wiley-VCH. (C) Amorphous IMC loaded into a CD-MOF to form IMC@CD-MOF composites, which resulted in a significant increase in solubility and bioavailability. Reproduced with permission from ref. 110. Copyright 2024 Elsevier. (D) A redox-responsive AIE-COF targeting hepatic macrophages for the treatment of drug-induced liver injury. Reproduced with permission from ref. 111. Copyright 2024 Wiley-VCH.

cancer immunotherapy. 109 Due to their superior biocompatibility, AIE-COFs show potential in enhancing antitumor immunity and providing precision intervention in cardiovascular treatments by integrating materials science, photomedicine, and immunological mechanisms.

Enhancing drug stability and improving real-time visualization of drug molecules are critical challenges in pharmaceutical sciences. Peng et al. demonstrated the unique AIE properties of indomethacin (IMC) solid-state fluorescent compounds and their potential in drug delivery. 110 By encapsulating amorphous IMC into a porous γ-cyclodextrin-based metal-organic framework (CD-MOF), they created IMC@CD-MOF composites, which exhibited significantly improved solubility and bioavailability compared to pure crystalline and amorphous IMC (Fig. 5(C)). Furthermore, the physical stability of IMC was enhanced in the MOF compared to pure amorphous drugs. The fluorescence properties of the IMC@CD-MOF allowed for direct visualization of drug molecular states, with significant fluorescence quenching indicating a non-aggregated, highenergy molecular state. This AIE-based imaging technique provides a highly sensitive and spatially resolved method for

monitoring drug delivery and stability in complex biological environments.

The increasing misuse of antipyretic and analgesic drugs has led to a surge in acute drug-induced liver injuries, highlighting the urgent need for precise and effective drug delivery systems. In response, Zhuang et al. developed a redox-responsive AIE-COF composite specifically targeting liver macrophages.<sup>111</sup> They synthesized two COFs (Se-COF and Se-BCOF) using diselenides, which possess dynamic exchange properties and low chemical bonding energies, making them ideal for drug delivery applications (Fig. 5(D)). These COFs were loaded with matrine and berberine, enabling dual-drug targeted delivery for the treatment of drug-induced liver injury. The loaded COFs inhibited the overactivation of reactive oxygen species (ROS) and the NLRP3/ASC/caspase-1 signaling pathway in damaged liver tissues while leveraging the protective effects of berberine to suppress JNK phosphorylation and nuclear Nrf-2 expression. This mechanism effectively mitigated liver inflammation and oxidative stress, offering a superior therapeutic alternative to conventional N-acetylcysteine (NAC) treatment.

integrating AIE-active molecules with frameworks such as MOFs and COFs, these composite materials achieve remarkable sensitivity and selectivity in bioimaging and clinical diagnostics. Additionally, they provide flexible and efficient solutions for targeted drug delivery, disease treatment, and mechanistic studies. With further advancements in synthesis techniques and safety evaluations, AIE-MOF/COF composites are expected to play a pivotal role in precision medicine and integrated therapeutic strategies, driving innovation in biomedical applications.

### 3.4 AIE-MOF/COF materials for photocatalysis and electrocatalysis

While the application of MOFs and COFs in photocatalysis has been extensively studied, the integration of AIE to enhance their photocatalytic performance—particularly in multi-modal catalysis-remains a relatively unexplored area. Recent research has demonstrated that incorporating AIEactive linkers into MOF/COF structures can improve photocatalytic efficiency by facilitating electron transfer, enhancing charge separation, and enabling multifunctional catalytic processes.112

Chen et al. designed and synthesized a tetraconnected AIE-active organic linker, H<sub>4</sub>-TPE<sub>4</sub>Pz, by combining a TPE core with a pyrazole moiety.113 Using this linker in combination with Ni<sub>8</sub> clusters as nodes, they assembled a (4,12)-connected MOF with an ftw-a topology (TPE<sub>4</sub>Pz-Ni), which exhibited remarkable chemical stability in various solvents and under strong alkaline conditions. Notably, the luminescence of TPE<sub>4</sub>Pz-Ni was significantly quenched due to ligand-to-metal charge transfer (LMCT) from the TPE core to the Ni<sub>8</sub> cluster (Fig. 6(A)). This material functioned as a photoredox/nickel dual catalyst in the C-S cross-coupling reaction between aryl iodides and thiols, demonstrating outstanding catalytic activity. Mechanistic studies revealed that the TPE<sub>4</sub>Pz unit acted as the photocapture center, while Ni<sub>8</sub> clusters served as catalytic centers, facilitating synergistic catalysis through electron and radical transfer. These findings highlight the potential of AIE-MOFs in organic transformations, expanding their applications in sustainable catalysis.

The detection and remediation of toxic pollutants, particularly heavy metals such as hexavalent chromium (Cr(vI)), remain significant challenges in water treatment. To address this, Li et al. developed a Tb@Zr-MOF composite by

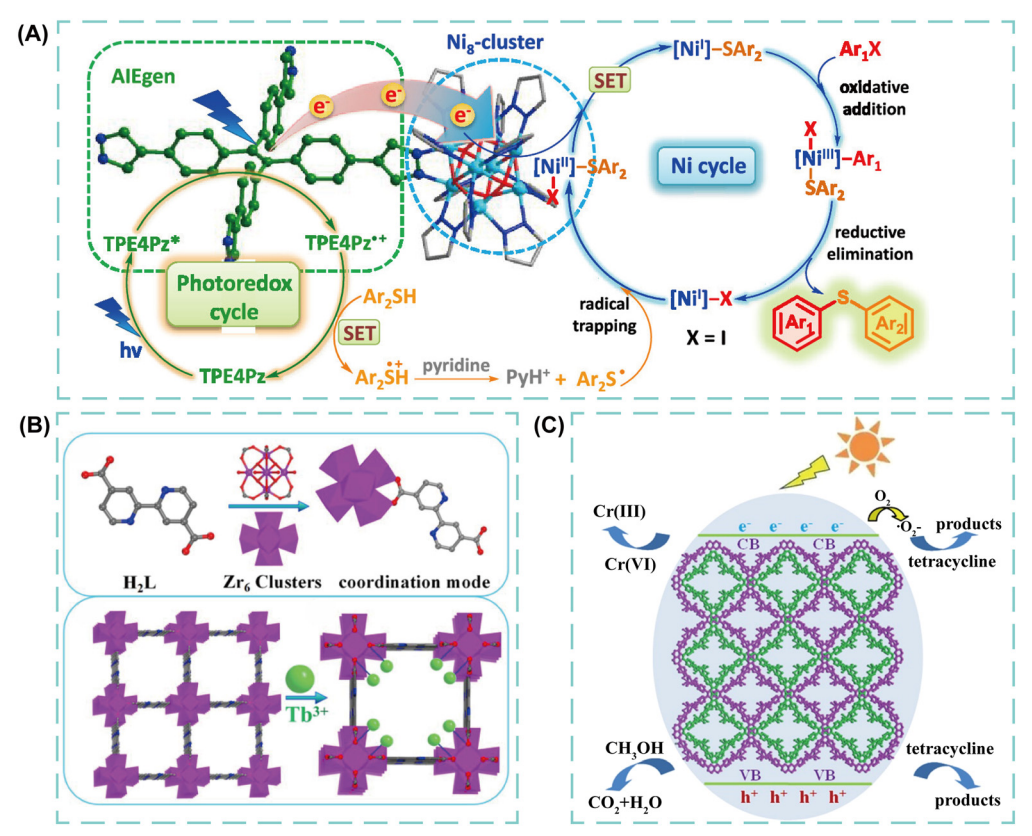


Fig. 6 (A) A TPE core with a pyrazole moiety formed an AIE-active linker. Combined with a Ni<sub>8</sub> cluster, the resulting MOF efficiently catalyzed the C-S cross-coupling of aryl iodides and thiols. Reproduced with permission from ref. 113. Copyright 2024 American Chemical Society. (B) A Tb@Zr-MOF composite material for effective reduction of Cr(vı) ions. Reproduced with permission from ref. 114. Copyright 2023 The Royal Society of Chemistry. (C) An AIE-MOF material with Cd(II) as the metal node has been synthesized, exhibiting highly sensitive fluorescence sensing performance for  $Cr_2O_7^{2-}$  in aqueous solution and a high photoreduction rate for  $Cr_2O_7^{2-}$  and tetracycline. Reproduced with permission from ref. 120. Copyright 2024 American Chemical Society.

integrating terbium (Tb3+) ions into a Zr-bipyridine MOF via post-modification techniques. 114 This composite exhibited unique dual-emission properties, with Tb<sup>3+</sup> ions emitting bright green fluorescence ( $\lambda_{max}$  = 546 nm), while the Zr-MOF exhibited blue-shifted fluorescence at 361 nm, with significantly reduced intensity (Fig. 6(B)). This dual-emission behavior enabled self-calibrated fluorescence sensing, enhancing detection accuracy for Cr(v1). Additionally, the Tb@Zr-MOF demonstrated exceptional photocatalytic activity, achieving a 97.5% reduction efficiency of Cr(vi) under UV irradiation. Theoretical calculations and experimental results indicated that Tb<sup>3+</sup> incorporation narrowed the band gap and lowered the conduction band potential of the Zr-MOF, effective facilitating electron-hole separation significantly boosting photocatalytic performance. Furthermore, the antenna effect between lanthanide ions and ligands improved luminescence demonstrating the multifunctionality of AIE-MOFs in sensing and pollutant degradation. 115-119

While significant progress has been made photocatalytic materials for single-pollutant treatment, the materials development of multi-modal simultaneously addressing multiple contaminants remains a key challenge. To tackle this issue, Guo et al. synthesized a water-stable Cd(II)-based MOF (CCSFU-1) using 2,3,6,7tetrakis(4-carboxyphenyl)quinoxaline (H<sub>4</sub>TCPQ) as the organic linker. 120 The tetraphenylquinoxaline moiety in CCSFU-1 exhibited AIE, enabling highly sensitive fluorescence sensing of  $\operatorname{Cr_2O_7^{2-}}$  in aqueous solutions. Besides sensing applications, the pore structure of CCSFU-1 facilitated the simultaneous adsorption and photocatalytic degradation of both  $\operatorname{Cr_2O_7}^{2-}$  and tetracycline, a widely used antibiotic pollutant (Fig. 6(C)). The photoreduction rate constants for Cr<sub>2</sub>O<sub>7</sub><sup>2-</sup> and tetracycline were measured to be 0.176 min<sup>-1</sup> and 0.0253 min<sup>-1</sup>, respectively, values that surpass those of most previously reported MOF-based photocatalysts. In addition, Zou et al. developed a redox-active Dy-MOF using a TPE-based ligand. 121 The material showed dual functionality in Cr(vI) detection (LOD: 11 nM) and visible-light-driven reduction (99.1% efficiency), enabled by effective ligand-tometal charge transfer and Dy-O active sites. These results suggest that modulating the crystalline structure of MOFs to harness the AIE effect provides a promising strategy for developing multifunctional photoactive materials for complex environmental remediation.

Electrocatalytic technology plays a significant role in the environment, new energy, and chemical synthesis. 122 However, the high cost and scarcity of traditional electrocatalytic materials, such as iridium, platinum, and ruthenium, have inhibited the large-scale application of electrocatalysis. Therefore, finding low-cost, stable, and highperformance electrocatalysts is an important challenge. Porous nanostructured catalysts, such as MOFs and COFs, which possess large surface areas, excellent stability, effective mass transfer ability, and easily adjustable catalytic binding potential sites, strong in the field

electrocatalysis.  $^{123,124}$  Recent studies on MOF/COF catalytic materials have shown interesting research in carbon dioxide reduction, water electrolysis,  $etc.^{125-128}$  However, many electrocatalytic intermediate reaction processes are still worth exploring. AIE materials have high probing ability, and Wang's research has utilized them for detecting poisonous  $NO_x$  by aggregation-induced electrochemiluminescence probes to reveal Pt catalyst deactivation and halide ion activation effects. The kinetics of  $NO_2$  intermediate formation during the electroreduction of nitrate to ammonia was investigated  $in\ situ$  on palladium nanoparticles with different crystallographic surfaces.  $^{129,130}$ 

AIE materials can be used to address the diminished photoelectrochemical utilization caused by stacking of conventional materials, as mentioned in the above article. However, whether it can also solve the decrease in electrocatalytic activity due to stacking is a question worth exploring. Metal porphyrins are widely used as homogeneous electrocatalysts. Nichols' group found that porphyrin aggregation under homogeneous conditions inhibits electrocatalysis, which can be modulated by titration of certain additives and modification of the ligand structure. 131 McCrory's group mitigated the limitation of catalytic activity aggregation by codepositing phthalocyanine(CoPc) with the coordination polymer poly(4vinylpyridine) (P4VP) on the electrode surface, which also provided additional catalytic enhancements. 132 Due to the properties of AIE materials, it is possible that they may also mitigate catalytic performance by counteracting  $\pi$ -stacking interactions. Although the thermal construction of AIE-MOF/ COF materials for electrocatalysis is rare, leveraging the porous structure of AIE-MOF/COF materials to improve the exposure probability of active sites and promote the charge transfer rate may be a feasible solution to address the challenges of reduced electrocatalysis.

AIE-MOF/COF materials possess tunable structures, high specific surface areas, and multifunctional capabilities, making them highly promising for advanced photocatalysis, electrocatalysis, or photoelectrocatalysis. In the future, the development of novel AIE molecules, optimization of MOF/COF structures, multi-functionalization, and large-scale production are expected to enhance their role in catalysis, offering new solutions for energy and environmental challenges.

### Conclusion and future perspectives

AIEgens enhance fluorescence efficiency by restricting intramolecular motion through coordination, covalent, or non-covalent bonding within MOF/COF materials. This restriction enables highly sensitive and accurate fluorescence analysis. These materials possess customizable optical properties and intrinsic porosity, making them ideal candidates for responsive devices. The structural rigidity and porosity of the frameworks further enhance their sensing

capabilities, allowing AIEgen-based luminescent porous materials to make significant strides across various fields.

Despite these advancements, several challenges and opportunities remain:

- 1. Understanding AIE mechanisms: while the RIM is a well-established mechanism of AIE, emerging AIE systems cannot be fully explained by RIM alone. A deeper and more comprehensive investigation into the underlying mechanisms governing AIE behavior is necessary for advancing material design.
- 2. Diverse linkers for enhanced design: most linkers used in constructing AIE-MOF/COF materials are based on TPE or its derivatives. Exploring alternative non-TPE-based linkers could open new avenues for innovation and broaden the design possibilities for porous AIE materials.
- 3. Sensitivity and selectivity: although AIE-MOF/COF materials have shown rapid progress in sensing applications, their performance in complex chemical environments is often hindered by interfering ions, leading to reduced detection sensitivity. Achieving high sensitivity and selectivity, particularly in biological settings, remains a critical challenge. The development of AIE-MOF/COF materials with superior selectivity, sensitivity, and stability in diverse microenvironments is essential.
- 4. Integration of multifunctional components: the inherent porosity of these frameworks allows for the incorporation of functional components such as metal ions, clusters, and quantum dots, which can further enhance the properties of AIE-MOF/COF materials. However, research in this area remains relatively limited, presenting vast opportunities for future exploration and innovation.
- 5. Sensing materials are expected to evolve towards realtime intelligent detection with integrated functions such as signal amplification, self-reporting, and adaptive response. AIE-MOF/COF materials hold great promise for point-of-care diagnostics and field monitoring. Future work will focus on enhancing stability, miniaturization, and compatibility with portable devices for smart, user-friendly sensing systems.

This review highlights the progress of AIE-MOF/COF materials in applications such as optical devices, sensing, biomedicine, and photocatalysis, with a focus on their luminescence properties and recent technological advancements. Additionally, it provides discussion on the structural functionalization of AIE-MOF/ COF materials to guide the future design of multifunctional materials. While the development of AIEgen-based porous materials is still in the early stages, their potential is vast, offering exciting challenges and opportunities for future advancements.

## Data availability

No primary research results, software or code have been included and no new data were generated or analysed as part of this review.

### Author contributions

All the authors together prepared this manuscript.

### Conflicts of interest

There are no conflicts to declare.

### Acknowledgements

This work was supported by the National Natural Science Foundation of China (No. 22279031), the Doctoral Research Foundation Project of Hubei University of Arts and Science (no. kygdf2020023), and the Hubei Key Laboratory of Low Dimensional Optoelectronic Material Devices (HLOM242012).

### Notes and references

- 1 J. Mei, N. L. C. Leung, R. T. K. Kwok, J. W. Y. Lam and B. Z. Tang, Chem. Rev., 2015, 115, 11718-11940.
- 2 M. Asad, M. Imran Anwar, A. Abbas, A. Younas, S. Hussain, R. Gao, L.-K. Li, M. Shahid and S. Khan, Coord. Chem. Rev., 2022, 463, 214539.
- 3 S. Cao, A. Thomas and C. Li, Angew. Chem., Int. Ed., 2023, **62**, e202214391.
- 4 C. Wang, S. Li, B. Qian, J. Sun, Z. He, Y. Wang, S. Zhang and C. Luo, Coord. Chem. Rev., 2024, 520, 216148.
- 5 Th. Förster and K. Kasper, Z. Phys. Chem., 1954, 1, 275–277.
- 6 W. Z. Yuan, P. Lu, S. Chen, J. W. Y. Lam, Z. Wang, Y. Liu, H. S. Kwok, Y. Ma and B. Z. Tang, Adv. Mater., 2010, 22, 2159-2163.
- 7 M. Huang, R. Yu, K. Xu, S. Ye, S. Kuang, X. Zhu and Y. Wan, Chem. Sci., 2016, 7, 4485-4491.
- 8 J. Luo, Z. Xie, J. W. Y. Lam, L. Cheng, B. Z. Tang, H. Chen, C. Qiu, H. S. Kwok, X. Zhan, Y. Liu and D. Zhu, Chem. Commun., 2001, 1740-1741.
- 9 J. Mei, Y. Hong, J. W. Y. Lam, A. Qin, Y. Tang and B. Z. Tang, Adv. Mater., 2014, 26, 5429-5479.
- 10 Y. Hong, J. W. Y. Lam and B. Z. Tang, Chem. Soc. Rev., 2011, 40, 5361.
- 11 J. Sun, H. Li, X. Gu and B. Z. Tang, Adv. Healthcare Mater., 2021, 10, 2101177.
- 12 J. Li, J. Wang, H. Li, N. Song, D. Wang and B. Z. Tang, Chem. Soc. Rev., 2020, 49, 1144-1172.
- 13 H. Wang and G. Liu, J. Mater. Chem. B, 2018, 6, 4029-4042.
- 14 K. Zhu, X. Xu and B. Yan, Acc. Mater. Res., 2024, 5, 1401-1414.
- 15 S. Daliran, A. R. Oveisi, Y. Peng, A. López-Magano, M. Khajeh, R. Mas-Ballesté, J. Alemán, R. Luque and H. Garcia, Chem. Soc. Rev., 2022, 51, 7810-7882.
- 16 J. Hyeon Kim, D. Won Kang, H. Yun, M. Kang, N. Singh, J. Seung Kim and C. Seop Hong, Chem. Soc. Rev., 2022, 51, 43-56.
- 17 K. Xu, S. Zhang, X. Zhuang, G. Zhang, Y. Tang and H. Pang, Adv. Colloid Interface Sci., 2024, 323, 103050.

18 R. Freund, O. Zaremba, G. Arnauts, R. Ameloot, G. Skorupskii, M. Dincă, A. Bavykina, J. Gascon, A. Ejsmont, J. Goscianska, M. Kalmutzki, U. Lächelt, E. Ploetz, C. S. Diercks and S. Wuttke, *Angew. Chem., Int. Ed.*, 2021, 60, 23975–24001.

Highlight

- 19 X. Ren, G. Liao, Z. Li, H. Qiao, Y. Zhang, X. Yu, B. Wang, H. Tan, L. Shi, X. Qi and H. Zhang, *Coord. Chem. Rev.*, 2021, 435, 213781.
- 20 M. Ma, X. Lu, Y. Guo, L. Wang and X. Liang, TrAC, Trends Anal. Chem., 2022, 157, 116741.
- 21 Y. Yang, C. Zhang, D. Cao, Y. Song, S. Chen, Y. Song, F. Wang, G. Wang and Y. Yuan, *Chem. Commun.*, 2024, 60, 2605–2612.
- 22 L. Ma, X. Feng, S. Wang and B. Wang, *Mater. Chem. Front.*, 2017, 1, 2474-2486.
- 23 L. Zhu, B. Zhu, J. Luo and B. Liu, *ACS Mater. Lett.*, 2021, 3, 77–89.
- 24 P. Ju, G. Zhang, W. Lu, S. Wang, A. Li, Q. Zhang, J. Xin, L. Shen, L. Jiang and E. Zhang, *Talanta*, 2024, 274, 126068.
- 25 X. Zhang, H. Dong, H. Zhou, Y. Li, Q. Liu, H. Cui, S. Wang, Y. Li and Q. Wei, *Sens. Actuators*, B, 2024, 400, 134911.
- 26 M. Xu, S. Tang, Z. Liu, W. Hou, J. Wu, R. Pan, C. Liu, W. Shen, S. Liang and H. K. Lee, *Talanta*, 2025, 283, 127125.
- 27 L. Wang, W. Chen, W. Song, J. Tian, J. Sun, L. Wen, C. Sun, X. Wang, Z. Su and G.-G. Shan, *Chin. Chem. Lett.*, 2023, 34, 107291.
- 28 J. Fang, Z. Fu, X. Chen, Y. Liu, F. Chen, Y. Wang, H. Li, Y. Yusran, K. Wang, V. Valtchev, S. Qiu, B. Zou and Q. Fang, Angew. Chem., Int. Ed., 2023, 62, e202304234.
- 29 S. S. Mohammed Ameen, N. M. Sher Mohammed and K. M. Omer, *Talanta*, 2023, 254, 124178.
- 30 X. Wen, C. Li, Z. Zhou, Y. He, J. He and X. Hou, *Talanta*, 2023, **265**, 124778.
- 31 H. Wang, X. Qian and X. An, *Int. J. Biol. Macromol.*, 2023, 251, 126363.
- 32 L. Zou, M. Li, X. Wang, M. Ye, L. Chen, L. Wang and Y. Song, *Spectrochim. Acta, Part A*, 2024, 311, 123978.
- 33 X.-Z. Guo, J. Zhang, B. Lin, G.-Z. Xiong, X.-X. Zhang, Z.-C. Li, L. Gui, Y. Si, S.-S. Chen and Z. Qiu, J. Mol. Struct., 2024, 1303, 137569.
- 34 W. Wei, H. Ze and Z. Qiu, *TrAC, Trends Anal. Chem.*, 2023, **161**, 116997.
- 35 Y. Cheng, X. Yin, D. Kukkar, J. Wang, K.-H. Kim and D. Zhang, *TrAC*, *Trends Anal. Chem.*, 2024, **180**, 117945.
- 36 S. Dalapati, C. Gu and D. Jiang, Small, 2016, 12, 6513-6527.
- 37 B. Z. Tang, X. Zhan, G. Yu, P. P. S. Lee, Y. Liu and D. Zhu, J. Mater. Chem., 2001, 11, 2974–2978.
- 38 G. v. Bünau, Ber. Bunsen-Ges., 1970, 74, 1294-1295.
- 39 F. Würthner, T. E. Kaiser and C. R. Saha-Möller, *Angew. Chem., Int. Ed.*, 2011, **50**, 3376–3410.
- 40 J. Wang, J. Mei, R. Hu, J. Z. Sun, A. Qin and B. Z. Tang, J. Am. Chem. Soc., 2012, 134, 9956–9966.
- 41 Y. Hong, J. W. Y. Lam and B. Z. Tang, *Chem. Commun.*, 2009, 4332–4353.
- 42 R. Hu, N. L. C. Leung and B. Z. Tang, *Chem. Soc. Rev.*, 2014, 43, 4494–4562.

- 43 Z. Shuang, Q. Anjun, S. Jingzhi and T. Benzhong, *Prog. Chem.*, 2011, 23, 623–636.
- 44 D. Ding, K. Li, B. Liu and B. Z. Tang, Acc. Chem. Res., 2013, 46, 2441–2453.
- 45 N. B. Shustova, B. D. McCarthy and M. Dincă, *J. Am. Chem. Soc.*, 2011, **133**, 20126–20129.
- 46 N. B. Shustova, T.-C. Ong, A. F. Cozzolino, V. K. Michaelis, R. G. Griffin and M. Dincă, J. Am. Chem. Soc., 2012, 134, 15061–15070.
- 47 J. Li, M. Xi, L. Hu, H. Sun, C. Zhu and W. Gu, *Anal. Chem.*, 2024, **96**, 2100–2106.
- 48 J. Zhang, S. Zhao, X. Tao, Q. Chen, D. Yin and C. Zhang, *Polyhedron*, 2024, **259**, 117067.
- 49 W. Xu, S. Xu, X. Zhang, K. Huang, L. Liang and D. Qin, Microchem. J., 2024, 207, 111866.
- 50 L. Zhang, X. Wang, X. Wang, X. Wang, Y. Luo, C. Tan, L. Jiang, Y. Wang and W. Liu, *Inorg. Chem.*, 2023, 62, 6421–6427.
- 51 J. Dong, P. Shen, S. Ying, Z.-J. Li, Y. D. Yuan, Y. Wang, X. Zheng, S. B. Peh, H. Yuan, G. Liu, Y. Cheng, Y. Pan, L. Shi, J. Zhang, D. Yuan, B. Liu, Z. Zhao, B. Z. Tang and D. Zhao, *Chem. Mater.*, 2020, 32, 6706–6720.
- 52 X. Xu, H. Lin, B. Lin, L. Huang, P. Wu, Y. Wu and L. Huang, *Anal. Chim. Acta*, 2023, 1277, 341681.
- 53 Y. Yang, W. Li, C. Sun, G. Shan, C. Qin, K. Shao, J. Wang and Z. Su, *Adv. Opt. Mater.*, 2022, **10**, 2200174.
- 54 M.-J. Dong, W. Li, Q. Xiang, Y. Tan, X. Xing, C. Wu, H. Dong and X. Zhang, ACS Appl. Mater. Interfaces, 2022, 14, 29599–29612.
- 55 C. Huang, M. Chen, L. Du, J. Xiang, D. Jiang and W. Liu, *Molecules*, 2022, 27, 8386.
- 56 Z. Wei, Z.-Y. Gu, R. K. Arvapally, Y.-P. Chen, R. N. Jr., J. F. Ivy, A. A. Yakovenko, D. Feng, M. A. Omary and H.-C. Zhou, *J. Am. Chem. Soc.*, 2014, 136, 8269–8276.
- 57 Q. Zhang, J. Su, D. Feng, Z. Wei, X. Zou and H.-C. Zhou, *J. Am. Chem. Soc.*, 2015, **137**, 10064–10067.
- 58 X. Guo, N. Zhu, S.-P. Wang, G. Li, F.-Q. Bai, Y. Li, Y. Han, B. Zou, X.-B. Chen, Z. Shi and S. Feng, *Angew. Chem., Int. Ed.*, 2020, 59, 19716–19721.
- 59 Y. Xin, D. Zhang, Y. Zeng, Y. Wang and P. Qi, *Anal. Methods*, 2023, 15, 788–796.
- 60 Y. Guo, J. Zhang, J. Liu, N. Wang and X. Su, *Anal. Chim. Acta*, 2023, **1276**, 341649.
- 61 T. Li, H. Zhu and Z. Wu, Nanomaterials, 2023, 13, 470.
- 62 T.-Y. Zhou, S.-Q. Xu, Q. Wen, Z.-F. Pang and X. Zhao, *J. Am. Chem. Soc.*, 2014, 136, 15885–15888.
- 63 Z.-F. Pang, S.-Q. Xu, T.-Y. Zhou, R.-R. Liang, T.-G. Zhan and X. Zhao, *J. Am. Chem. Soc.*, 2016, **138**, 4710–4713.
- 64 Z.-F. Pang, T.-Y. Zhou, R.-R. Liang, Q.-Y. Qi and X. Zhao, *Chem. Sci.*, 2017, **8**, 3866–3870.
- 65 S. Dalapati, E. Jin, M. Addicoat, T. Heine and D. Jiang, J. Am. Chem. Soc., 2016, 138, 5797–5800.
- 66 C. Huang, S. Zhou, C. Chen, X. Wang, R. Ding, Y. Xu, Z. Cheng, Z. Ye, L. Sun, Z. Wang, D. Hu, X. Jia, G. Zhang and S. Gao, *Small*, 2022, 18, 2205062.
- 67 Y. Tang, M. Zheng, W. Xue, H. Huang and G. Zhang, ACS

- Appl. Mater. Interfaces, 2022, 14, 37853-37864.
- 68 W. Gong, Y. Dong, C. Liu, H. Shi, M. Yin, W. Li, Q. Song and C. Zhang, Dyes Pigm., 2022, 204, 110464.
- 69 G. Lin, H. Ding, D. Yuan, B. Wang and C. Wang, J. Am. Chem. Soc., 2016, 138, 3302-3305.
- 70 G. Lin, H. Ding, R. Chen, Z. Peng, B. Wang and C. Wang, J. Am. Chem. Soc., 2017, 139, 8705-8709.
- 71 H. Ding, J. Li, G. Xie, G. Lin, R. Chen, Z. Peng, C. Yang, B. Wang, J. Sun and C. Wang, Nat. Commun., 2018, 9, 5234.
- 72 H. Yuan, X. Xu, Z. Qiao, D. Kottilil, D. Shi, W. Fan, Y. D. Yuan, X. Yu, A. Babusenan, M. Zhang and W. Ji, Adv. Opt. Mater., 2024, 12, 2302405.
- 73 J. Liu, X. Jin, X. Li, X. Ma, P. Cui, T. Zhang, W. Chen and W. Huang, Chem. Commun., 2025, 61, 5341-5344.
- 74 M. Liu, Y.-Z. Cheng, Y. Fu, S. Bi, X. Ding, B.-H. Han, Q. Xu and G. Zeng, Chin. J. Chem., 2025, 43, 633-640.
- 75 H. Wan, X. Wang, Q. Nie, X. Wang, L. Wang and Y. Song, Adv. Opt. Mater., 2025, 13, 2402907.
- 76 V. Kachwal, S. Mollick and J.-C. Tan, Adv. Funct. Mater., 2024, 34, 2308062.
- 77 S. Jindal, J.-X. Wang, Y. Wang, S. Thomas, A. Mallick, M. Bonneau, P. M. Bhatt, O. Alkhazragi, I. Nadinov, T. K. Ng, O. Shekhah, H. N. Alshareef, B. S. Ooi, O. F. Mohammed and M. Eddaoudi, J. Am. Chem. Soc., 2024, 146, 25536-25543.
- 78 X. Zhu, Y. Wang, T. He, S. Thomas, H. Jiang, O. Shekhah, J.-X. Wang, T. K. Ng, H. N. Alshareef, O. M. Bakr, B. S. Ooi, M. Eddaoudi and O. F. Mohammed, J. Am. Chem. Soc., 2025, 147, 6805-6812.
- 79 C. Jia, T. He and G.-M. Wang, Coord. Chem. Rev., 2023, 476, 214930.
- 80 S. Kamal, M. Khalid, M. S. Khan and M. Shahid, Coord. Chem. Rev., 2023, 474, 214859.
- 81 F.-Y. Ye, M. Hu and Y.-S. Zheng, Coord. Chem. Rev., 2023, 493, 215328.
- 82 L. Zhang, X. Bi, H. Wang, L. Li and T. You, Talanta, 2024, 273, 125843.
- 83 Z. Yan, L. Fang, Z. He, H. Xie, B. Liu, B. Guo and Y. Yao, Small, 2022, 18, 2200388.
- 84 Q. Li, X. Wu, X. Huang, Y. Deng, N. Chen, D. Jiang, L. Zhao, Z. Lin and Y. Zhao, ACS Appl. Mater. Interfaces, 2018, 10, 3801-3809.
- 85 W.-M. Chen, J.-J. Shao, Y. Zhang, Z.-D. Xue, P.-L. Liu, J.-L. Ni and F.-M. Wang, J. Coord. Chem., 2023, 76, 1394-1404.
- 86 W. Liu, P. Zheng, Y. Xia, F. Li and M. Zhang, Talanta, 2024, 269, 125352.
- 87 Y. Liao, L. Hu, J. Huang, J. Liu, P. Li and S. Zhang, Spectrochim. Acta, Part A, 2024, 307, 123617.
- 88 Y. Lu, L. Yu, S. Zhang, P. Su, X. Li, X. Hao, S. Wang and M. Sun, Appl. Surf. Sci., 2023, 625, 157202.
- 89 D. Wei, M. Li, Y. Wang, N. Zhu, X. Hu, B. Zhao, Z. Zhang and D. Yin, J. Hazard. Mater., 2023, 441, 129890.
- 90 Y. Tang, M. Zheng, W. Xue, H. Huang and G. Zhang, ACS Appl. Mater. Interfaces, 2022, 14, 37853-37864.
- 91 H. Zhu, B. Liu, J. Pan, L. Xu, J. Liu, P. Hu, D. Du, Y. Lin and X. Niu, Biosens. Bioelectron., 2025, 267, 116756.

- 92 T. Wang, L. Wang, G. Wu and D. Tian, Sens. Actuators, B, 2024, 399, 134867.
- 93 J. Tang, T. Cai, N. Li, Z. Chen, J. Liu and H. Yang, J. Hazard. Mater., 2025, 491, 137964.
- 94 Y. Jiang, W. Chang, Z. Li, X. Zhou, P. Zhang, X. Huang, X. Pan, Z. He, Y. Wang and Z. Tian, JACS Au, 2025, 5, 1875-1883.
- 95 P. Peng, M. Li, X. Wang, M.-J. Dong, Y. Xiao, F. Ahmad, T. Hou, T. Shu and X. Zhang, Anal. Chem., 2025, 97, 2153-2163.
- 96 R. Isci, B. Can Sadikogullari, B. Sütay, B. Karagoz, A. Daut Ozdemir and T. Ozturk, J. Photochem. Photobiol., A, 2025, 459, 116095.
- 97 Q. Liu, D. Wang, Y. Yang, Y. Zhu, Y. Zou, M. Wang, L. Li, E. R. Thomas, X. Li, Y. Xiao, Y. Li, X. Zhou, D. Gao and J. Wu, Biosens. Bioelectron., 2025, 276, 117244.
- 98 F. Gao, M. Liu, W. Wang, J. Lou, Y. Chang and N. Xia, Spectrochim. Acta, Part A, 2025, 325, 125088.
- 99 N. Feng, X. Huang, Y. Zhao, Q. Wang, X. Peng, Y. Dong, L. Xue, B. Z. Tang and Y. Chen, Adv. Funct. Mater., 2025, 35, 2410900.
- 100 L. Zhang, S.-C. Wan, J. Zhang, M.-J. Zhang, Q.-C. Yang, B. Zhang, W.-Y. Wang, J. Sun, R. T. K. Kwok, J. W. Y. Lam, H. Deng, Z.-J. Sun and B. Z. Tang, J. Am. Chem. Soc., 2023, 145, 17689-17699.
- 101 F. Yuan, C. Zhang, X. Luo, X. Shen and Y. Xian, Chem. Commun., 2023, 59, 5122-5125.
- 102 P. Rana, D. Dabur and H.-F. Wu, Mater. Today Chem., 2024, 38, 102074.
- 103 B. Gao, K. Yang, M. Yang, W. Li, T. Jiang, R. Gao, Y. Pei, Z. Pei and Y. Lv, Chem. Commun., 2024, 60, 8892-8895.
- 104 H. Li, Y. Hao, Z. Zhang, L. Liu, H. Wang, H. Ma and Q. Wei, Chem. Eng. J., 2024, 500, 156813.
- 105 J. Li, T. Wu, X. Liu, R. Feng, Y. Du, F. Li and Q. Wei, Anal. Chem., 2024, 96, 18170-18177.
- 106 S. Hu, L. Xu, M. Huang, Y. Wu, X. Qin and B. Deng, Sens. Actuators, B, 2025, 424, 136925.
- 107 C. Li, Z. Yang, J. Wang, H. Cheng, J. Liu, Y. Ding and J. Zhu, Adv. Funct. Mater., 2025, 2504380.
- 108 L. Zhang, F. Guo, S. Xu, Q. Deng, M. Xie, J. Sun, R. T. K. Kwok, J. W. Y. Lam, H. Deng, H. Jiang, L. Yu and B. Z. Tang, Adv. Mater., 2023, 2304620.
- 109 L. Zhang, B. Zhang, M.-J. Zhang, W. Li, H. Li, Y. Jiao, Q.-C. Yang, S. Wang, Y.-T. Liu, A. Song, H.-T. Feng, J. Sun, R. T. K. Kwok, J. W. Y. Lam, B. Z. Tang and Z.-J. Sun, Nat. Commun., 2025, 16, 44.
- 110 Y. Peng, Y. Lei, J. Luo, X. Hu, F. Sun, Y. Yang, M. Guo and T. Cai, Chem. Eng. J., 2024, 479, 147654.
- 111 J. Zhuang, H. Zhang, J. Wu, D. Hu, T. Meng, J. Xue, H. Xu, G. Wang, H. Wang and G. Zhang, Small, 2024, 20, 2402656.
- 112 Q. Liu, D. Li, X. Lei, Y. Chen, J. Wang, A. Liu, B. Han and G. He, Sep. Purif. Technol., 2023, 310, 122938.
- 113 Y. Chen, C. Li, X. Wang, L. Fan, Y. Zhang, X. Zhao, Q.-Y. Li and X.-J. Wang, Inorg. Chem., 2024, 63, 19924-19930.
- 114 Q. Li, Z.-Q. Wu, D. Li, T.-H. Liu, H. Yin, X.-B. Cai, W. Zhu, Z.-L. Fan and R.-Z. Li, J. Mater. Chem. A, 2023, 11, 2957-2968.

115 Y. Xie, G. Sun, G. A. Mandl, S. L. Maurizio, J. Chen, J. A. Capobianco and L. Sun, *Angew. Chem., Int. Ed.*, 2023, **62**,

Highlight

- e202216269.

  116 J. Chen, M. Li, R. Sun, Y. Xie, J. R. Reimers and L. Sun, *Adv. Funct. Mater.*, 2024, 34, 2315276.
- 117 H.-Q. Yin, X.-Y. Wang and X.-B. Yin, *J. Am. Chem. Soc.*, 2019, **141**, 15166–15173.
- 118 F. Liu, W. Zhou, X. Li, Z. Li, S. Lu, X. Shang, C. Tan, P. Hu, Z. Chen and X. Chen, *Talanta*, 2023, 262, 124729.
- 119 S. Xu, G. Xiong, X.-Y. Zhang, K. Huang, D.-B. Qin and B. Zhao, *Cryst. Growth Des.*, 2023, 23, 4214–4221.
- 120 S. Mi, L. Wang, H. Guo, Y. Su, S. Wang, J. Xu, J. Cao and X. Guo, *Cryst. Growth Des.*, 2024, 24, 405–413.
- 121 W. Zou, Q. Li, Q. Wu, Z. Zhang and Y. Zhou, Chem. Eng. J., 2025, 505, 159428.
- 122 G. Yang, Q. Xu and G. Zeng, Electron, 2024, 2, e39.
- 123 H. Wang, X. Wang, Y. Jiang, M. Li, H. Peng, G. Ma, L. Zhu, I. Shakir and Y. Xu, *Chem. Rec.*, 2025, e202400244.
- 124 N. Sun, S. S. A. Shah, Z. Lin, Y.-Z. Zheng, L. Jiao and H.-L. Jiang, *Chem. Rev.*, 2025, 125, 2703–2792.

- 125 Q. Zhou, X. Wang, S. Rong, G. Li, Q. Jiang, H. Pang and H. Ma, *Inorg. Chem.*, 2025, 64, 5291–5301.
- 126 G. Das, S. Singha Roy, F. Abou Ibrahim, A. Merhi, H. N. Dirawi, F. Benyettou, A. Kumar Das, T. Prakasam, S. Varghese, S. Kumar Sharma, S. Kirmizialtin, R. Jagannathan, F. Gándara, S. Aouad, M. A. Olson, S. Kundu, B. R. Kaafarani and A. Trabolsi, *Angew. Chem.*, 2025, 137, e202419836.
- 127 T. Huang, L.-P. Sun, X. Li and B.-O. Guan, *Adv. Mater.*, 2025, 37, 2411510.
- 128 Q. Wang, J. Chen, H. Pan, W. Liu, Y. Liu, B. Chen, D. Qi, K. Wang and J. Jiang, *Adv. Mater.*, 2025, 2502644.
- 129 D. Sun, J. Zhang, J. Du, Y. Yin and B. Wang, Chem. Eng. J., 2025, 510, 161608.
- 130 D. Sun, J. Du, Y. Yin, J. Zhang, W. Deng, W. Lv and B. Wang, *Chem. Eng. J.*, 2025, **508**, 160763.
- 131 K. L. Branch, E. R. Johnson and E. M. Nichols, *ACS Cent. Sci.*, 2024, **10**, 1251–1261.
- 132 W. S. Dean, T. L. Soucy, K. E. Rivera-Cruz, L. L. Filien, B. D. Terry and C. C. L. McCrory, *Small*, 2025, 21, 2402293.